



Published in final edited form as:

J Acoust Soc Am. 2006 December ; 120(6): EL63–EL69.

Acoustic response from adherent targeted contrast agents

Shukui Zhao, Dustin E. Kruse, Katherine W. Ferrara, and Paul A. Dayton

Department of Biomedical Engineering, University of California, Davis, California 95616,
kwferrara@ucdavis.edu

Abstract

In ultrasonic molecular imaging, encapsulated micron-sized gas bubbles are tethered to a blood vessel wall by targeting ligands. A challenging problem is to detect the echoes from adherent microbubbles and distinguish them from echoes from non-adherent agents and tissue. Echoes from adherent contrast agents are observed to include a high amplitude at the fundamental frequency, and significantly different spectral shape compared with free agents ($p < 0.0003$). Mechanisms for the observed acoustical difference and potential techniques to utilize these differences for molecular imaging are proposed.

1. Introduction

Although the oscillation of cavitation bubbles near a boundary^{1–3} and the dynamics of an encapsulated gas bubble far from a boundary⁴ have been studied extensively, a unique problem arises when encapsulated micron-sized gas bubbles attach to a vessel wall and are insonified in medical ultrasound applications. In ultrasonic molecular imaging, micron-sized gas bubbles are coated with a shell that supports peptide- or antibody-based targeting ligands, where these ligands bind to receptors on a blood vessel wall. Thus, tethers on the order of nanometers in length connect these small bubbles to endothelial cells and bring them in close contact with a boundary. The oscillation of these adherent microbubbles was observed to be asymmetrical by high-speed photography⁵ but their acoustic response has not been reported previously. Optimal detection of bound agents would require differentiating their echoes from those produced by freely circulating agents and the surrounding tissue.⁶ Detection of the echoes from small bubbles tethered to the endothelium is a challenging problem since the quantity of microbubbles retained at a target site is small, and their signal can be easily masked by the background from freely circulating non-adherent agents.^{7,8}

Ultrasound radiation force can facilitate binding between the agents and target site, increase the number of adherent agents available for imaging, and reduce the waiting period for accumulation of targeted agents.^{9,10} Augmenting radiation force for bubble localization with signal processing schemes based on acoustic characteristics to differentiate free and bound agents could then produce a rapid and efficient molecular imaging scheme.

In this manuscript, we report in-vitro observations for the echo spectra of adherent and freely flowing contrast agents. By combining optical and acoustical experimental systems, a protocol was developed to force microbubbles to bind to a phantom vessel wall using radiation force, with the binding verified optically, and the echo spectra recorded acoustically. Differences in the acoustical response between free and bound contrast agents are observed, and possible mechanisms for these differences are examined with evidence from optical experiments and simulations. We conclude with proposed methods to specifically detect bound targeted contrast agents based on differences in their scattered echo spectrum.

2. Methods

2.1 Optical experiments

Optical experiments were performed to observe the effect of an ultrasound radiation force pulse and localization of targeted microbubble on a vessel wall. The experimental setup has been described in detail previously.⁹ In short, a 200- μm cellulose tube was placed at the mutual focus of a 60x objective and a single element transducer (V3966, OD 0.75 inch and ID 0.47 inch, Panametrics-NDT, Waltham, MA). The radiation force pulse was at 4 MHz and ~ 50 kPa, and the microbubble concentration was ~ 4000 microbubbles per microliter. After application of 10 radiation force pulses, the tube was scanned up and down by adjusting the focal plane and images of adherent microbubbles were saved.

2.2 Acoustical Experiment

A custom two-element coaxial and confocal transducer facilitated the recording of the fundamental frequency and higher harmonics. Specifically, a 2.25 MHz outer annular element (V3966, OD 0.75 inch and ID 0.47 inch, Panametrics-NDT, Waltham, MA) was used for transmission and a 15 MHz inner element (IM1502HR, 0.25 inch, Valpey Fisher Corp., Hopkinton, MA) was used for reception, each with a one inch focal length (Figure 1). The one-way -6 dB bandwidth was $\sim 120\%$ (0.9 to 3.6 MHz) and 90 % (~ 10 to 23 MHz) for the outer and inner elements respectively. The excitation pulse was either a Blackman-windowed 10-cycle pulse with a center frequency of 4 MHz or a 5-cycle pulse with a center frequency of 2 MHz with matched pressure and intensity generated on an arbitrary wave generator (AWG 2021, Tektronix, Inc., Beaverton, OR). The received echoes were amplified 40 dB with a Panametrics receiver (5900PR, Panametrics-NDT, Waltham, MA), digitized by a 12-bit A/D board (PDA12A, Signatec Inc, Corona, CA) configured to sample at 125 MHz, and analyzed offline via Matlab (v7.1, The Mathworks Inc, Natick, MA).

A 200- μm inner diameter cellulose microtube was placed at the focus of both transducer elements, and a solution of targeted microbubbles (~ 4000 microbubbles per microliter) was pumped through the tube with a mean velocity of 10 mm/s. The microtube was held vertically to reduce bubble accumulation along the wall due to floatation and the transducer was placed at an angle of about 45 degrees to eliminate reflected echoes from the tube wall. The preparation of the targeted microbubbles and avidin-coated microtube have been described previously.⁹ Echoes were recorded from the contrast agents for a peak negative pressure (PNP) of 40, 130, 210, and 290 kPa. Acoustic calibration was performed with a needle hydrophone (PZT-0400, Onda Corp, Sunnyvale, CA) placed at the transducer focus. Freely flowing microbubbles were imaged first, followed by the application of 20 radiation force pulses. Each radiation force pulse consisted of 5 million cycles at 4 MHz and a PNP of ~ 50 kPa, promoting the adhesion of targeted agents to the tube wall. Optical observation confirmed bubble adhesion. Free contrast agents were then rinsed from the tube and echoes from the remaining adherent bubbles were acquired. Data were averaged over 10 sets for adherent microbubbles and 33 sets for freely flowing agents.

2.3 Simulation

Simulations were carried out to investigate the effect of coherent echo summation due to the localization of contrast agents on a vessel wall. In these simplified simulations, microbubbles are assumed to be of the same size (1.2 microns in diameter), and either randomly distributed inside a vessel (free) or localized on one portion of a vessel wall within a 90-degree angle (adherent). The echo from the 1.2-micron microbubble driven by a 10-cycle Blackman-windowed pulse at 4 MHz and 210 kPa was calculated from a modified Rayleigh-Plesset equation¹¹ and summed for every microbubble according to their spatial positions. The diameter of the vessel was varied from 200 to 20 microns. The same number of microbubbles

was involved for the free and adherent cases. Simulations were repeated 20 times for each case and statistical mean and standard deviations of the received echo power were reported in log scale.

3. Results

3.1 Experiments

No adherent microbubbles were observed on the tube wall before the radiation force pulse and approximately 100 adherent microbubbles were observed within a tube length of 100 μm after deflection. Some of the adherent microbubbles formed aggregates separated by $\sim 20 \mu\text{m}$ or less (Figure 2). Adherent microbubbles were spatially distributed on the side of the vessel wall away from the transducer.

With the wideband 15 MHz element used for echo reception, higher order harmonics were observed up to 20 MHz. Spectra shown in Figure 3 were obtained using a PNP of 210 kPa, averaged over 10 sets for bound contrast agents and over 33 sets for freely circulating agents, and then converted into dB using a reference voltage of 1 mV. The spectral intensity at fundamental and harmonic frequencies was quantified by calculating the average intensity within a 1-MHz frequency band centered at different frequencies.

The fundamental spectral intensity increased 14 to 22 dB for bound agents compared with free agents with transmission at 2 and 4 MHz ($p < 0.0001$ and 0.0003 respectively) (Figure 4). The second harmonic component also increased for bound relative to free agent echoes following transmission with a center frequency of 2 MHz at all four pressure levels ($p < 0.0001$ for PNP = 40, 130, 210 kPa and $p < 0.001$ for PNP = 290 kPa) and was significantly changed for transmission of 4 MHz at two pressure levels ($p < 0.0001$ and 0.0006 for PNP = 40 and 130 kPa, respectively). Higher harmonic components increased as a result of the radiation force pulse only for 2 MHz transmission at 130 kPa ($p < 0.003$ and 0.005 for 3rd and 4th harmonic, respectively, data not shown).

The echo spectrum from freely circulating agents demonstrates small differences between the fundamental echo intensity and the intensity of the 2nd and 3rd harmonic components; less than 6 dB and 10 dB for transmission center frequencies of 2 and 4 MHz, respectively (Figure 5a and 5b). In contrast, the difference between the fundamental intensity and the intensity of the 2nd and 3rd harmonic components for adherent agents can approach 18 dB and 30 dB, for 2 and 4 MHz transmission, respectively. For all cases studied here, the difference between the fundamental intensity and 2nd and 3rd harmonics of free agents was significantly smaller than this difference when computed for adherent agents ($p < 0.0001$).

3.2 Simulation

A significant difference in received echo power was observed between uniformly distributed free microbubbles in a vessel and adherent microbubbles localized on a vessel wall for vessels with a diameter larger than 20 microns (Figure 6). For a vessel with a diameter of 200 microns as in the experiments, an echo power from microbubbles localized along the vessel wall was ~ 20 dB higher than that for randomly distributed microbubbles ($p < 0.0001$). This difference becomes smaller (12 dB and 4 dB) but is significant for vessels with diameters of 100 and 50 microns, respectively ($p < 0.0001$), but not significant for a 20-micron vessel ($p = 0.86$).

4. Discussion and conclusions

The physical problem under investigation bears similarities to and differences from previous studies of cavitation bubble dynamics. In optical studies, the adherent microbubbles were observed to oscillate asymmetrically and form liquid jets,⁵ similar to bubbles in cavitation

studies. However, these targeted microbubbles are coated with a lipid shell, are tethered to a wall by ligands instead of simply in the proximity of the boundary, and are excited by an ultrasound pulse in the MHz frequency range. Additionally, the goal is to detect the echoes from adherent microbubbles and distinguish them from echoes from non-adherent microbubbles and tissue. Boundary integral method and image method^{2,12} used to simulate the dynamics of a cavitation bubble near a boundary may be adopted for these adherent microbubbles, although special care must be given to the adhesion between a microbubble and vessel wall and the effect of the bubble shell.

Two significant differences were observed between the echo spectrum of adherent microbubbles and that of free microbubbles, i.e., a significantly increased echo intensity at fundamental frequency and a significantly larger difference between the echo intensity at fundamental frequency and harmonics for adherent agents. We hypothesize three possible mechanisms for these experimentally observed differences.

First, when microbubbles are freely flowing in solution, their small diameter (less than $1/100^{\text{th}}$ of an acoustic wavelength) and nearly uniform spatial distribution result in incoherent echo summation and a small backscattered intensity from each sample volume. Alternatively, a layer of contrast agents adherent to the inside of a vessel wall reflects ultrasound coherently, resulting in a large reflection of the fundamental component (Figure 6). The formation of layers of perfluorocarbon nanoparticle contrast agents has also been reported to substantially increase their echogenicity over that observed when in solution.¹³

Second, optical observations indicated that adherent microbubbles formed aggregates (Figure 2), which increases the coupling between adjacent agents and the effective scattering cross section. Secondary radiation force is responsible for the nonuniform microbubble distribution.¹⁴ It has been demonstrated previously that aggregates of microbubbles produce a more narrowband response with higher amplitude at the fundamental frequency,¹⁵ and that microbubbles in close proximity couple acoustically and produce a harmonic response that is different from that produced by individual bubbles.¹⁶

Third, Zhao et al observed previously that microbubbles adherent to a vessel wall oscillate asymmetrically in the plane normal to the boundary, in contrast to free microbubbles which oscillate symmetrically.⁵ Further, for a low transmission pressure, the volume oscillation was observed to decrease in comparison with free agents. Asymmetrical oscillation of a cavitation bubble and formation of a jet near an elastic boundary, a curved or flat rigid boundary, or within a vessel have been studied both theoretically and experimentally by number of research groups.^{1-3,17} The effect of the decreased volume oscillation on the echo spectrum is the subject of future studies.

Finally, we note that our study involved the averaged echo spectrum over a pulse train. The largest spectral difference between adherent and free microbubbles is observed at 210 kPa for 4 MHz and ~ 130 kPa for 2 MHz, while the difference is smaller at the highest pressure of 290 kPa (Figure 4 and 5). Decrease in signal power was also observed during acoustic experiments at 290 kPa and more noticeable at 2 MHz than 4 MHz. Optical studies (not shown) and these acoustical changes demonstrate that some of the adherent bubbles may be fragmented and the number of available adherent agents is decreasing at 290 kPa.

Regardless of the mechanisms responsible, the difference in spectral characteristics between bound and free contrast agents may be exploited in an imaging technique. Specifically, the application of imaging before and after a long, low amplitude pulse (designed to rapidly enhance the adhesion of targeted contrast agents) can be used to detect bound contrast agents. Given that echoes from the surrounding tissue should not change after the low amplitude radiation force pulse, the substantial spectral change before and after the radiation force pulse

will facilitate the differentiation of tissue and bound agent echoes. Following the radiation force pulse, an increase in the spectral intensity at the fundamental frequency likely indicates the presence of bound agents. Characterization of the ratio of fundamental intensity to harmonics before and after the radiation force pulse can also be used to indicate the presence of adherent agents. Further studies will examine the implementation of specific targeted bubble detection techniques.

Acknowledgements

This work is supported by the National Institutes of Health through the NIH Roadmap for Medical Research, Grant # R21EB005325-01, as well as R21CA098692, T32EB003827, R01CA 112356, and R01CA103828.

References

1. Tomita Y, Robinson PB, Tong RP, et al. "Growth and collapse of cavitation bubbles near a curved rigid boundary,". *J Fluid Mech* 2002;466:259–283.
2. Sato K, Tomita Y, Shima A. "Numerical-Analysis of a Gas Bubble near a Rigid Boundary in an Oscillatory Pressure Field,". *J Acoust Soc Am* 1994;95(5):2416–2424.
3. Brujan EA, Nahen K, Schmidt P, et al. "Dynamics of laser-induced cavitation bubbles near an elastic boundary,". *J Fluid Mech* 2001;433:251–281.
4. Church CC. "The effects of an elastic solid surface layer on the radial pulsations of gas-bubbles,". *J Acoust Soc Am* 1995;97(3):1510–1521.
5. Zhao SK, Ferrara KW, Dayton PA. "Asymmetric oscillation of adherent targeted ultrasound contrast agents,". *Appl Phys Lett* 2005;87(13):134103.
6. Christiansen JP, Lindner JR. "Molecular and cellular imaging with targeted contrast ultrasound,". *P IEEE* 2005;93(4):809–818.
7. Schumann PA, Christiansen JP, Quigley RM, et al. "Targeted-microbubble binding selectively to GPIIb IIIa receptors of platelet thrombi,". *Invest Radiol* 2002;37(11):587–593. [PubMed: 12393970]
8. Leong-Poi H, Christiansen J, Klibanov AL, et al. "Noninvasive assessment of angiogenesis by ultrasound and microbubbles targeted to alpha(v)-integrins,". *Circulation* 2003;107(3):455–460. [PubMed: 12551871]
9. Zhao S, Borden M, Bloch SH, et al. "Radiation-force assisted targeting facilitates ultrasonic molecular imaging,". *Mol Imaging* 2004;3(3):135–148. [PubMed: 15530249]
10. Rychak JJ, Klibanov AL, Hossack JA. "Acoustic radiation force enhances targeted delivery of ultrasound contrast microbubbles: in vitro verification,". *IEEE Trans Ultrason Ferroelectr Freq Control* 2005;52(3):421–433. [PubMed: 15857050]
11. Morgan KE, Allen JS, Dayton PA, et al. "Experimental and theoretical evaluation of microbubble behavior: Effect of transmitted phase and bubble size,". *IEEE Trans Ultrason Ferroelectr Freq Control* 2000;47(6):1494–1509.
12. Krasovitski B, Kimmel E. "Gas bubble pulsation in a semiconfined space subjected to ultrasound,". *J Acoust Soc Am* 2001;109(3):891–898. [PubMed: 11303943]
13. Lanza GM, Troustil RL, Wallace KD, et al. "In vitro characterization of a novel, tissue-targeted ultrasonic contrast system with acoustic microscopy,". *J Acoust Soc Am* 1998;104(6):3665–3672. [PubMed: 9857523]
14. Dayton PA, Morgan KE, Klibanov ALS, et al. "A preliminary evaluation of the effects of primary and secondary radiation forces on acoustic contrast agents,". *IEEE Trans Ultrason Ferroelectr Freq Control* 1997;44(6):1264–1277.
15. Dayton PA, Morgan KE, Klibanov AL, et al. "Optical and acoustical observations of the effects of ultrasound on contrast agents,". *IEEE Trans Ultrason Ferroelectr Freq Control* 1999;46(1):220–232.
16. Allen JS, Kruse DE, Dayton PA, et al. "Effect of coupled oscillations on microbubble behavior,". *J Acoust Soc Am* 2003;114(3):1678–1690. [PubMed: 14514221]
17. Hu YT, Qin SP, Hu T, et al. "Asymmetric oscillation of cavitation bubbles in a microvessel and its implications upon mechanisms of clinical vessel injury in shock-wave lithotripsy,". *Int J Nonlinear Mech* 2005;40(2–3):341–350.

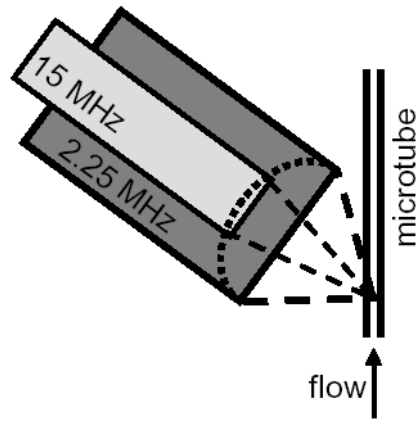


Fig. 1.
Experimental diagram.

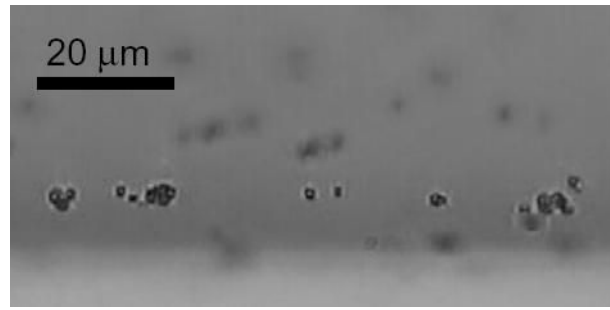


Fig. 2. Optical observation of adherent microbubbles on a vessel wall and formation of aggregates.

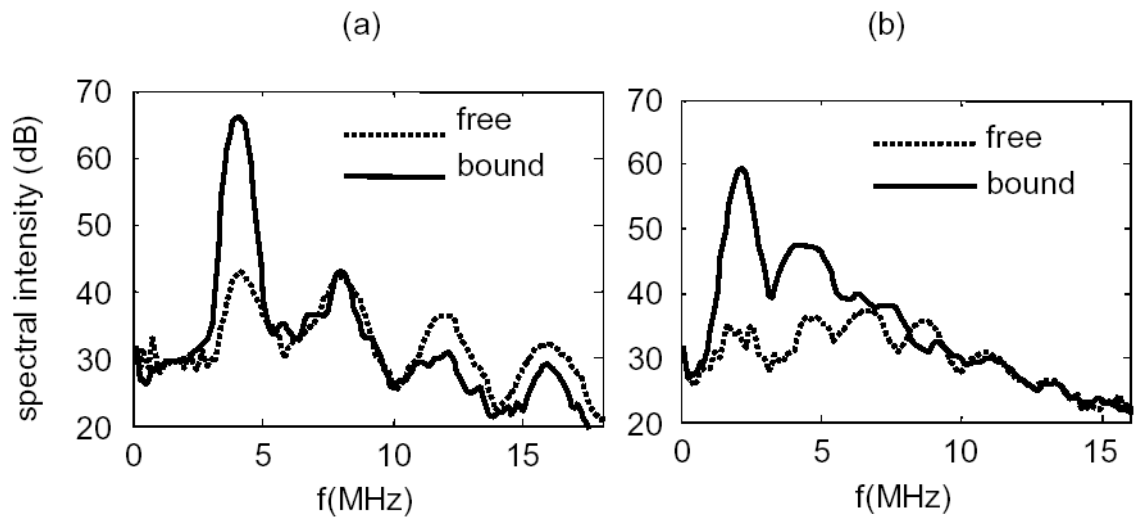


Fig. 3. Spectral intensity for echoes from free and bound microbubbles following transmission with a PNP of 210 kPa and a center frequency of 4 MHz (a) and 2 MHz (b).

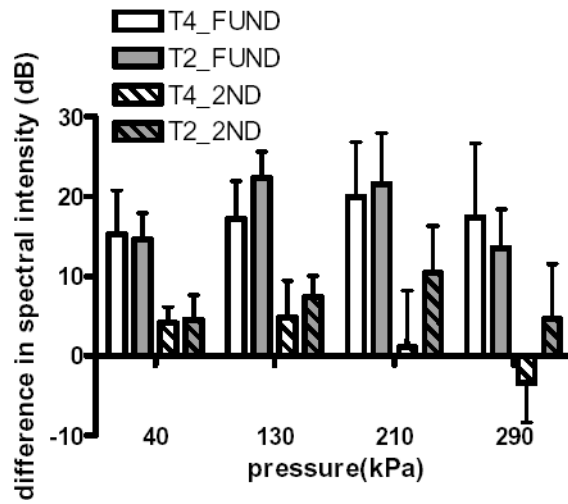


Fig. 4. Difference in spectral intensity at the fundamental (plain) and second harmonic (striped) frequency between bound and free agents, following transmission with a center frequency of 2 MHz (gray) or 4 MHz (white).

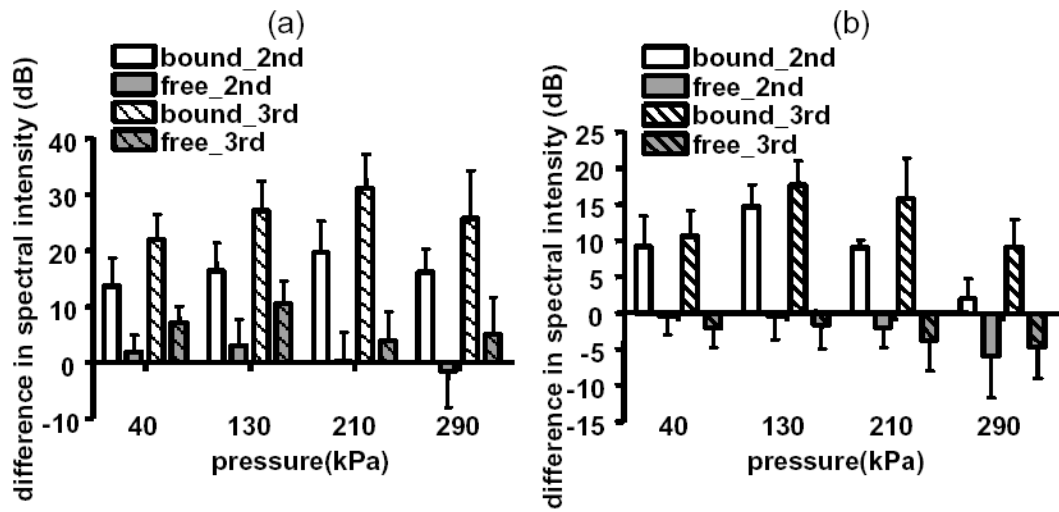


Fig. 5. Difference in echo spectral intensity of the second (plain) and third harmonic (striped) relative to the fundamental component for bound and free agents following transmission at 4 MHz (a) and at 2 MHz (b).

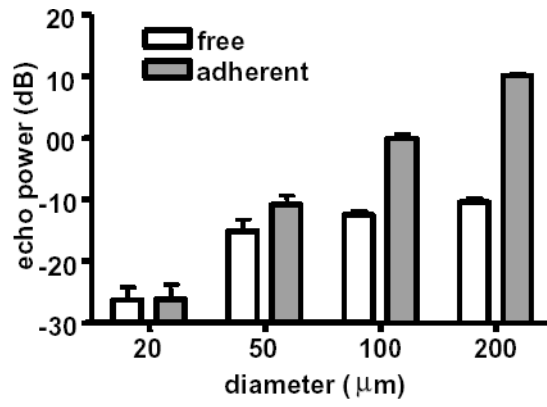


Fig. 6. Echo power from simulated free and adherent agents in different size vessels.